

Hydration of Barium Monohydroxide in (H₂O)₁₋₃ Clusters: Theory and Experiment

Iván Cabanillas-Vidoso^{a)}, Maximiliano Rossa^{b)}, Gustavo A. Pino^{b)}, Juan C. Ferrero^{b)*}
and Carlos J. Cobos^{a)**}

^a *Instituto de Investigaciones Fisicoquímicas Teóricas y Aplicadas (INIFTA),
Universidad Nacional de La Plata. Casilla de Correo 16, Sucursal 4, La Plata (1900),
Argentina*

^b *Centro Láser de Ciencias Moleculares, INFIQC, Departamento de Fisicoquímica,
Facultad de Ciencias Químicas, Universidad Nacional de Córdoba, Córdoba
(X5000IUS), Argentina*

Authors to whom correspondence should be addressed:

* J. C. Ferrero - Tel.: +54 351 4334169/80. FAX: +54 351 4334188 - e-mail:
jferrero@fcq.unc.edu.ar

** C. J. Cobos - Tel.: +54 221 4257291/7430. FAX: +54 221 4254642 - e-mail:
cobos@inifta.unlp.edu.ar

ABSTRACT

The ionization energies (IE_e 's) of small $BaOH(H_2O)_m$ clusters ($m = 1-3$), as generated in a laser vaporization-supersonic expansion source have been determined by laser photoionization experiments over the 3.65–4.55 eV energy range. Complementary *ab initio* studies show that the IE_e 's are in good agreement with computed adiabatic ionization energies, and that $BaOH(H_2O)_m$ structures with a direct coordination of the Ba atom to water molecules are favored over those that are characterized by H-bonded networks involving H_2O molecules and the OH group of BaOH. Additional calculations have been performed on the hydration energies for the most stable isomers of the relevant $BaOH(H_2O)_{1-3}$ clusters. A comparison is made between the closed-shell title system and the results of related theoretical studies on the open-shell alkali monohydroxides, which allows for an interpretation of the opposite trends that are found in the cluster size dependence of the vertical ionization energies for both series of systems, and highlights the role of the BaOH unpaired electron in its ionization process. Altogether, the present evidence suggests for the initial steps of the BaOH hydration process to be dominated by electrostatic and polarization interactions between the Ba^+ and OH^- ion cores, which become both increasingly solvated upon sequential addition of water molecules.

KEYWORDS: Solvation / Water clusters / Alkaline-earth containing radicals / Ionization energies / Ab initio calculations

1. Introduction

Over the last twenty years, research related to the hydration of metal atoms and ions has largely benefitted from the increasing potentiality of gas phase spectroscopy and mass spectrometry to probe a variety of solvation phenomena and the related chemistry of metal-doped water clusters.¹⁻⁴ In particular, a considerable interest on group 2 of metals have aroused due to their divalent nature that allows only one intermediate charge state, M^+ , between the stable neutral metal, M , and the doubly-charged M^{2+} ions, which are present in solutions.³ Many aspects of the structure, energetics, and reactivity of $M(H_2O)_n$ ($M = Mg, Ca, Ba$),⁵⁻⁷ $M^+(H_2O)_n$ ($M = Mg, Ca, Sr$),⁸⁻¹¹ and $M^{2+}(H_2O)_n$ ($M = Mg, Ca, Sr, Ba$)^{12,13} clusters have been explored at the molecular level from the experimental and theoretical viewpoints, leading to a case study of the stepwise microhydration of different metal oxidation states. In these studies, the formation of bare and hydrated MOH and MOH^+ products has been reported, as a result of reactions that occur either during the cluster formation process^{6,8-11} or upon their subsequent photoionization,⁵ photodissociation,⁸⁻¹¹ and collision-induced dissociation.¹² For the former case, the investigation of the hydration of a metal atom/ion or a MOH/MOH^+ radical in $(H_2O)_n$ clusters through cluster size-resolved experiments is feasible. Recent results on the hydration and reactions of neutral barium atoms in water clusters from this laboratory, provide a case in point.⁶ A series of experiments and *ab initio* calculations has been conducted to show that, as a result of distinct cluster-growing processes involving ground-state and electronically excited state Ba atoms, $Ba(H_2O)_n$ ($n = 1-4$) and $BaOH(H_2O)_m$ ($m = 1-3$) clusters are produced with similar abundances in a laser vaporization-supersonic expansion source. This was taken in the present study as an advantage point to investigate the stepwise hydration in water clusters of the $BaOH$ radical.

The relevance of the title system relies on the open-shell nature of BaOH, which distinguishes it from closed-shell, stoichiometric $\text{MOH}(\text{H}_2\text{O})_m$ ($M = \text{Li, Na, K, Rb, Cs}$)¹⁴⁻¹⁸ and $\text{MOH}^+(\text{H}_2\text{O})_m$ ($M = \text{Mg, Ca}$)^{19,20} systems that have been studied previously. Owing to the neutral charge state of BaOH and the highly ionic character of its Ba–OH bond, it will be significant to contrast the present results with those obtained in studying the hydration process of the related MOH ($M = \text{alkaline metal}$) species,¹⁴⁻¹⁸ in order to address the role of the BaOH unpaired electron on its stepwise hydration in small water clusters.

In this paper we report ionization energies for $\text{BaOH}(\text{H}_2\text{O})_m$ ($m = 1-3$) clusters determined by laser one-photon ionization experiments. Complementary high level *ab initio* calculations show that the experimental values are in good agreement with a chiefly adiabatic ionization process, and allows for interpreting the nature and energetics of the BaOH hydration structures, which are formed under the prevailing experimental conditions. A comparison is made between the title system and the results of related theoretical studies on the alkali monohydroxides,¹⁴⁻¹⁸ which allows for an interpretation of the opposite trends that are found in the cluster size dependence of the vertical ionization energies for both series of systems, as well as addressing the similarities and differences between the corresponding stepwise hydration behaviors.

2. Experimental details

The experimental setup has been fully described in previous works.^{6,7,21} Briefly, neutral $\text{BaOH}(\text{H}_2\text{O})_m$ clusters were generated in a pick-up source combining 1064 nm laser vaporization [(0.7 – 1.4) J cm⁻² laser fluence] of a rotating Ba disk, with a supersonic expansion of a gaseous He : H₂O (0.988 : 0.012) mixture through a pulsed solenoid valve (400 μm diameter) at a stagnation pressure of 2 bar. The molecular beam

of clusters was collimated with a 4.0 mm diameter skimmer placed 10 cm downstream from the nozzle, before entering into the ionization region of a differentially pumped Wiley-McLaren time-of-flight mass spectrometer (TOF-MS).

The one-photon ionization of the $\text{BaOH}(\text{H}_2\text{O})_m$ clusters was performed through the frequency-doubled output of a dye laser (0.04 cm^{-1} bandwidth), which was pumped by the second harmonic (532 nm) of a pulsed Nd:YAG laser. The ionization energy was varied by scanning the dye laser in steps of 0.02 eV over the 272.5–340.0 nm (4.55–3.65 eV) range. Some experiments were also performed with the fourth harmonic (266 nm) of the same Nd:YAG laser as the ionization source.

The photoions were detected by dual microchannel plates (MCP) and the MCP output signal was digitized and afterwards processed in a personal computer. An average of 512 events was used to generate the mass spectra, which were further normalized to the ionization laser power, as recorded on a relative basis by a photomultiplier tube. It was observed that the integrated intensity of any given $\text{BaOH}(\text{H}_2\text{O})_{n+1}$ cluster remains almost constant at energies near the IE threshold of $\text{BaOH}(\text{H}_2\text{O})_n$. This fact was used to normalize the mass spectra of the corresponding $\text{BaOH}(\text{H}_2\text{O})_n$ cluster, as the $\text{BaOH}(\text{H}_2\text{O})_n/\text{BaOH}(\text{H}_2\text{O})_{n+1}$ ratio, to determine the ionization energy of $\text{BaOH}(\text{H}_2\text{O})_n$. Numerical integration of the mass signals corresponding to the $\text{BaOH}^+(\text{H}_2\text{O})_m$ ($m = 1 - 3$) clusters then led to the relevant photoionization yield curves.

The electric field in the TOF-MS ionization region ($E_z = 192 \text{ V cm}^{-1}$) reduces the apparent ionization energy of the clusters by $2e(eE_z)^{1/2}$.^{7,21} Hence, a correction factor of 0.01 eV was applied to the experimental IE values.

3. Theoretical methods

As shown in a previous study addressing to neutral and cationic barium atom-water clusters,⁷ a good agreement between experimental and theoretical ionization energies was obtained by combining the *m*PW1PW91 method of the density functional theory (DFT)²² to derive optimized structures and harmonic vibrational frequencies and the high correlated coupled cluster singles and doubles excitations approach, including a perturbational estimate of the triples, CCSD(T, Full)^{23,24} to compute accurate total energies. In a similar way, in the present study the energetics of the neutral and cationic BaOH(H₂O)_{*m*} (*m*=0-3) species was derived from single-point CCSD(T, Full) calculations on *m*PW1PW91 geometries, using for both methods the relativistic effective core potential (RECP) developed by Lim *et al.*²⁵ for Ba and the split-valence 6-311++G(d,p) basis sets for the O and H atoms. All of the calculations were performed by using the Gaussian 09 suite of programs.²⁶

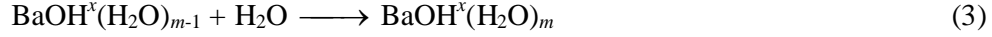
To analyze the stability of the barium monohydroxide–water clusters, total binding energies [$\Delta E_0(m)$] for the hydration processes BaOH^{*x*}+*m* H₂O → BaOH^{*x*}(H₂O)_{*m*} (with *x* = 0 for neutral and *x* = +1 for cationic clusters), were estimated as:

$$\Delta E_0(m) = E_0[\text{BaOH}^x(\text{H}_2\text{O})_m] - E_0[\text{BaOH}^x] - m E_0[\text{H}_2\text{O}] \quad (1)$$

where $E_0[\text{BaOH}^x(\text{H}_2\text{O})_m]$, $E_0[\text{BaOH}^x]$ and $E_0[\text{H}_2\text{O}]$ denote the CCSD(T, Full) total electronic energies of the relevant species, including zero-point vibrational energy (E_{ZPE}) corrections based on the *m*PW1PW91 calculations.

As usual, vertical ionization energies (IE_v) were computed as the total electronic energy difference, including E_{ZPE} corrections, between the cationic and neutral species, taken both at the optimized geometries of the neutral clusters. In a similar way, adiabatic ionization energies (IE_a) were derived from the optimized geometries of the cationic and the corresponding neutral clusters.

Additional calculations have been performed to evaluate the hydration energies (E_{hyd} 's) of both Ba- and BaOH-doped water clusters, as defined by the reactions



and calculated according to the expressions:

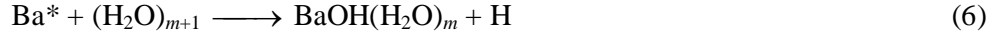
$$E_{\text{hyd}}(n) = E_0[\text{Ba}^x(\text{H}_2\text{O})_n] - E_0[\text{Ba}^x(\text{H}_2\text{O})_{n-1}] - E_0[\text{H}_2\text{O}] \quad (4)$$

$$E_{\text{hyd}}(m) = E_0[\text{BaOH}^x(\text{H}_2\text{O})_m] - E_0[\text{BaOH}^x(\text{H}_2\text{O})_{m-1}] - E_0[\text{H}_2\text{O}] \quad (5)$$

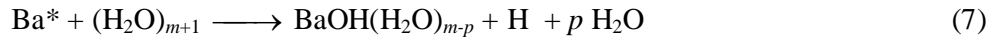
where $E_0[\text{Ba}^x(\text{H}_2\text{O})_n]$ is the energy of $\text{Ba}^x(\text{H}_2\text{O})_n$ clusters. The optimized geometries for the most stable $\text{Ba}(\text{H}_2\text{O})_n$ ($n = 0 - 4$) isomers were taken from Ref. 7.

4. Experimental results

The formation of $\text{BaOH}(\text{H}_2\text{O})_m$ clusters in the reaction of electronically excited Ba atoms with water clusters (Equation 6), has been recently demonstrated.⁶



The internal energy excess of the resulting barium monohydroxide-water clusters may be released in the early stages of the supersonic expansion, through collisions with He and by the following evaporative process:



Since the pick-up process occurs mostly in the post-expansion region, where the probability of multiple collisions with the buffer gas is low, the evaporation of water molecules is likely the dominant stabilization process for neutral $\text{BaOH}(\text{H}_2\text{O})_m$ clusters.

All of the observed $\text{BaOH}^+(\text{H}_2\text{O})_m$ ions arise from one-photon ionization of the corresponding neutral clusters that are entrained in the molecular beam, *i.e.*,



Considering that the calculated energies for the $\text{BaOH}^+(\text{H}_2\text{O})_m \rightarrow \text{BaOH}^+(\text{H}_2\text{O})_{m-1} + \text{H}_2\text{O}$ process are 1.03, 0.93, and 0.88 eV for $m = 1, 2,$ and $3,$ respectively, the evaporative photoionization of neutral $\text{BaOH}(\text{H}_2\text{O})_m$ species can be neglected so fragmentation-free photoionization is assumed under the prevailing, near-threshold ionization conditions.

Figure 1 shows the photoionization yield curves for the $\text{BaOH}(\text{H}_2\text{O})_{1-3}$ clusters. As in the case of $\text{Ba}(\text{H}_2\text{O})_{1-4},$ ⁷ the lowest post-threshold breaks in the logarithmic plot of the ion yield as a function of the photon energy (Watanabe-type plots) were assigned to the IE_e 's for the various $\text{BaOH}(\text{H}_2\text{O})_m$ clusters. The resulting values, which represent the average of three individual measurements, are listed in Table I. The associated uncertainty of 0.05 eV accounts for the deviation of these measurements, and includes an estimate of the error arising from the fact that the photoionization energy was varied in steps of 0.02 eV. Higher-energy breaks can be also observed in Figure 1 for $\text{BaOH}^+(\text{H}_2\text{O})_{2,3}.$ The corresponding IE_e values are listed in Table I.

As can be seen in Table I, all of the IE_e 's for $\text{BaOH}(\text{H}_2\text{O})_m$ ($m = 1 - 3$) are smaller than the value of (4.55 ± 0.03) eV that was previously determined for bare $\text{BaOH}.$ ¹⁶ In addition, these IE_e 's decrease systematically with the increasing size m of the cluster. This behavior is quite similar to that observed previously for $\text{Ba}(\text{H}_2\text{O})_{1-4}$ clusters.⁷ Yet, the observation of two lowest and close IE_e 's for both $\text{BaOH}(\text{H}_2\text{O})_2$ and $\text{BaOH}(\text{H}_2\text{O})_3$ species might be rationalized in a number of ways, including the presence in the molecular beam of either nearly isoenergetic isomers, or two low-lying vibrational states of a given isomer for such clusters. To elucidate this, *ab initio* calculations of stable structures, binding energies and vertical and adiabatic ionization energies were performed.

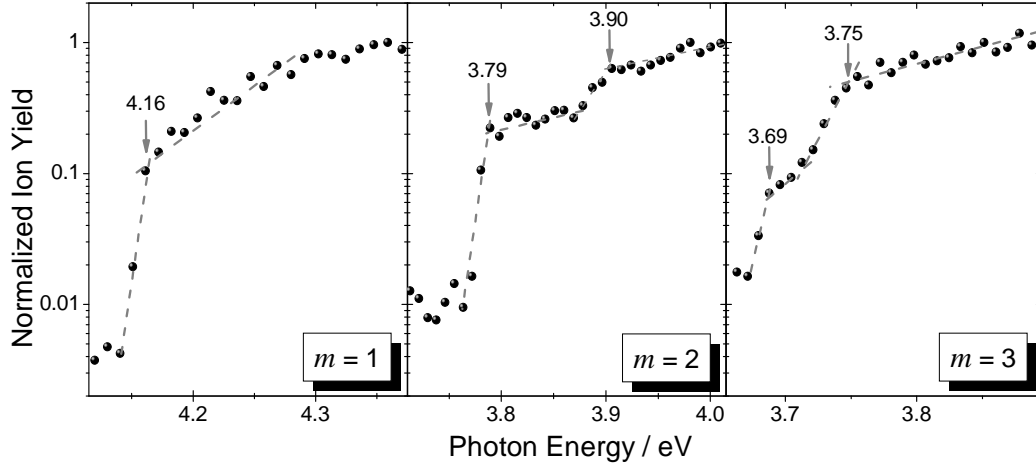


Figure 1. Photoionization yield curves for $\text{BaOH}(\text{H}_2\text{O})_m$ clusters. The position of the lower breaks associated with the IE_e 's are indicated by arrows.

Table I. Experimental and calculated vertical and adiabatic ionization energies for $\text{BaOH}(\text{H}_2\text{O})_m$ ($m = 0 - 3$). Selected hydration structures are highlighted (see text for details).

| $\text{BaOH}(\text{H}_2\text{O})_m$ | IE_e | Ionization Energy (eV) | | | | | |
|-------------------------------------|------------------------------------|--------------------------------|--------------------------------------|---------|--------------------------------------|---------------|-------------|
| | | Neutral Structure ^a | IE_v | | Ionic structure ^b | IE_a | |
| | | | DFT | CCSD(T) | | DFT | CCSD(T) |
| $m = 0$ | 4.55 ± 0.03^c | <i>BaOH</i> | 4.60 | 4.58 | <i>BaOH</i> ⁺ | 4.55 | 4.54 |
| $m = 1$ | 4.17 ± 0.05 | <i>1U01</i> | 4.38 | 4.36 | <i>1U01</i> ⁺ | 4.28 | 4.28 |
| | | <i>1U10</i> | 4.13 | 4.05 | <i>1U11</i> ⁺ | 4.09 | 4.01 |
| | | <i>1U11</i> | 4.35 | 4.32 | <i>1U11</i> ⁺ | 4.20 | 4.14 |
| $m = 2$ | 3.80 ± 0.05 3.91 ± 0.05 | <i>2U02</i> | 4.81 | 4.77 | <i>2U01</i> ⁺ | 4.37 | 4.38 |
| | | <i>2U20</i> | 3.95 | 3.80 | <i>2U21</i> ⁺ | 3.78 | 3.63 |
| | | <i>2U11</i> | 4.25 | 4.21 | <i>2U21</i> ⁺ | 4.00 | 3.87 |
| | | <i>2U22</i> | 4.10 | 4.06 | <i>2U22</i> ⁺ | 3.94 | 3.84 |
| $m = 3$ | 3.70 ± 0.05 3.76 ± 0.05 | <i>3U02</i> | 4.72 | 4.70 | <i>3U01_b</i> ⁺ | 4.47 | 4.50 |
| | | <i>3U23</i> | 4.02 | 3.98 | <i>3U23</i> ⁺ | 3.75 | 3.68 |
| | | <i>3U12_a</i> | 4.04 | 4.01 | <i>3U22_a</i> ⁺ | 3.81 | 3.70 |
| | | <i>3U20</i> | 4.00 | 3.80 | <i>3U21_b</i> ⁺ | 3.47 | 3.31 |
| | | <i>3U11</i> | 4.20 | 4.17 | <i>3U21_a</i> ⁺ | 3.73 | 3.50 |
| | | <i>3U12_b</i> | 4.00 | 3.96 | <i>3U32_a</i> ⁺ | 3.62 | 3.55 |
| | | <i>3U22</i> | 4.00 | 3.95 | <i>3U22_b</i> ⁺ | 3.80 | 3.73 |
| | | <i>3D33</i> | 3.97 | 3.95 | <i>3U33</i> ⁺ | 3.70 | 3.54 |
| <i>3U32</i> | 3.89 | 3.79 | <i>3U32_b</i> ⁺ | 3.66 | 3.53 | | |

^aSee neutral clusters in Figure 2. ^bSee ionic clusters in Figure 3. ^cExtracted from Ref. 21.

5. Theoretical results

5.1. BaOH radical

The calculated geometry of the BaOH radical agrees very well with previous experimental and theoretical values.²¹ The linear structure is well reproduced and the computed Ba-O bond distance of 2.204 Å is in excellent agreement with the experimental value of 2.201 Å.²⁷ The similarity of the neutral and cationic BaOH geometries leads to similar vertical and adiabatic IE's of 4.58 and 4.54 eV, respectively, which are also in very good agreement with the recent experimental determination of $(4.55 \pm 0.03 \text{ eV})$.²¹

Figures 2 and 3 show the optimized structures of BaOH and BaOH⁺, respectively, along with the corresponding charge distributions, as estimated employing a natural population analysis treatment. It is evident from these results that both species are strongly polarized as Ba⁺(OH)⁻ and Ba²⁺(OH)⁻.

5.2. Solvation of BaOH in water clusters

Figure 2 shows the *m*PW1PW91 optimized conformations of BaOH(H₂O)_{*m*} (*m* = 0 - 3) and the computed ΔE_0 values at the CCSD(T,Full) level of theory. As expected, the number of minimum energy structures increases significantly as the number of water molecules increases.

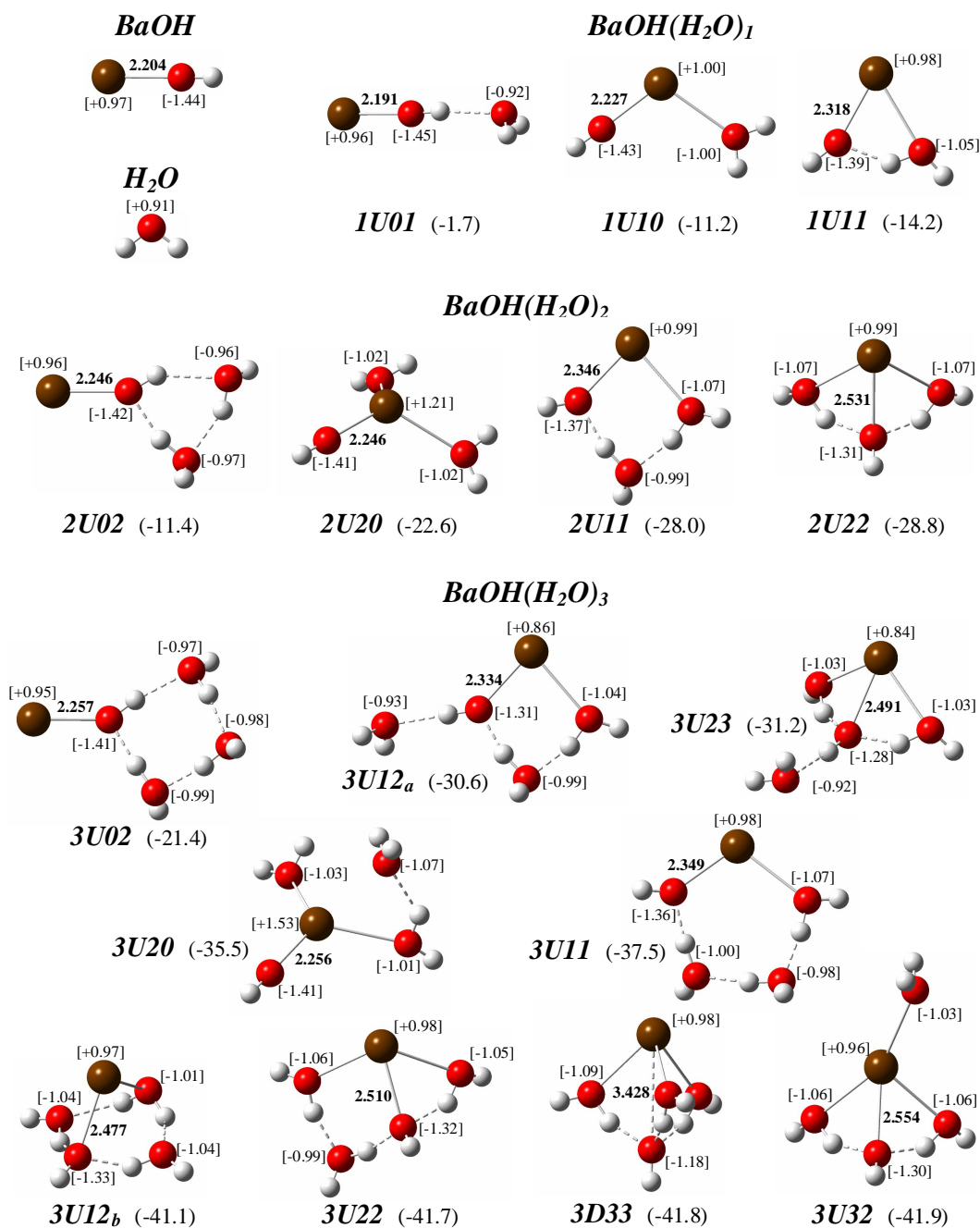


Figure 2. Optimized structures of neutral $\text{BaOH}(\text{H}_2\text{O})_m$ ($m = 0 - 3$) clusters calculated at the $m\text{PW1PW91}$ level. Binding energies (in kcal mol^{-1}) calculated at the $\text{CCSD}(\text{T},\text{Full})$ level are given under each structure. The Ba–OH lengths (R_0) are given in angstroms and the natural population analysis evaluated at DFT level are indicated between brackets.

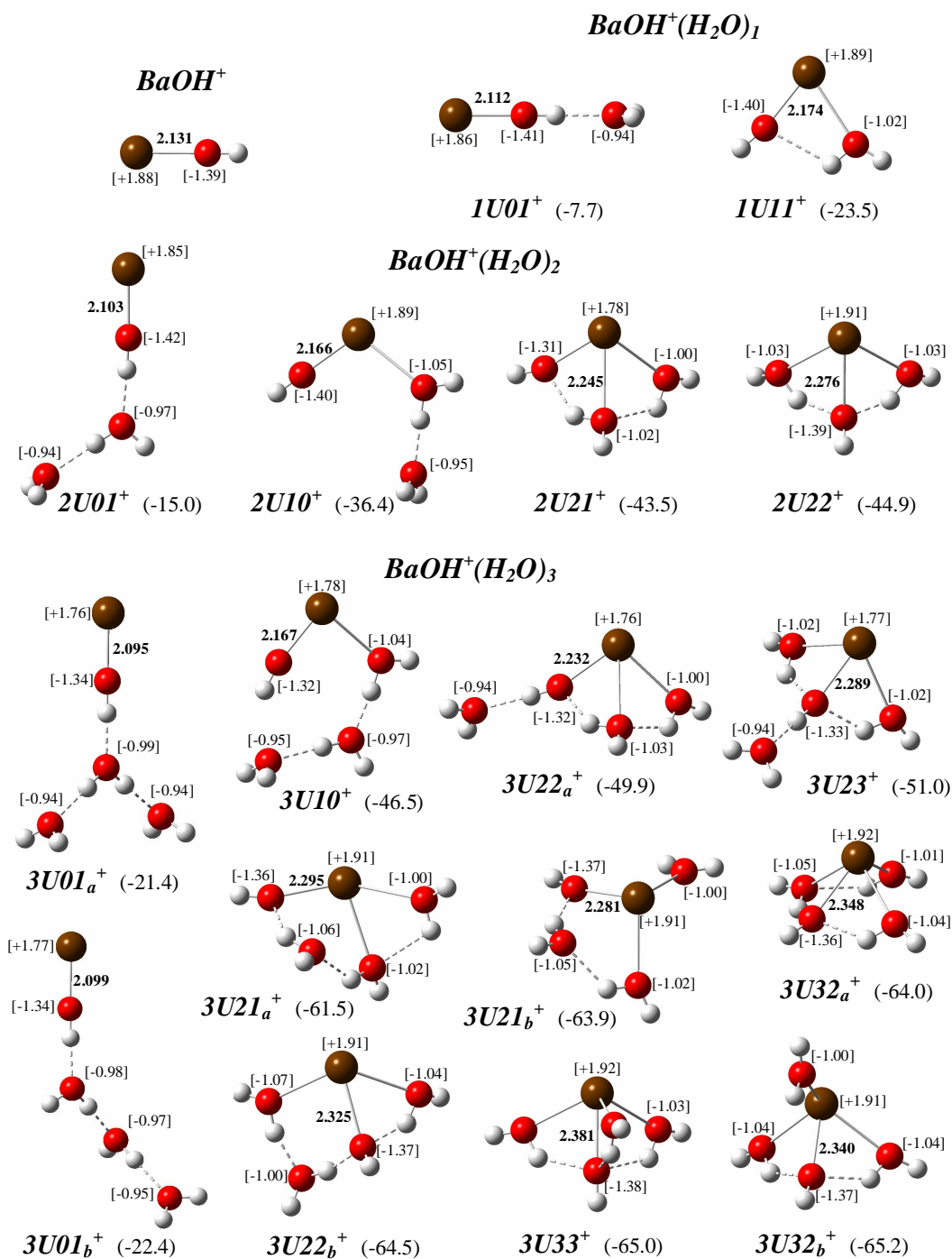


Figure 3. Same as Fig. 2, but for ionic BaOH⁺(H₂O)_m (m = 0 - 3) clusters.

In a previous study on $\text{Ba}(\text{H}_2\text{O})_n$ clusters,⁷ the different isomers were classified according to the number of water molecules present in the first, second, third, and fourth hydration shells of the Ba atom. For the present system, it is necessary instead to distinguish between the water molecules that are bonded to the Ba atom from those bonded to the OH group of BaOH. Hence, we used here the notations “ $mUwy_i$ ” and “ $mDwy_i$ ” proposed by Kim *et al.*,¹⁴⁻¹⁷ where m is the total number of water molecules, w and y are the hydration numbers of Ba and OH, respectively, U/D indicates the undissociated/dissociated state of Ba-OH, and the subscript i distinguishes among different conformers of the same isomer.

Three stable structures were found for $\text{BaOH}(\text{H}_2\text{O})_1$. The most stable isomer, $IUII$, presents both H_2O and OH bounded to Ba and has a binding energy of $\Delta E_0 = -14.2 \text{ kcal mol}^{-1}$. The O–Ba–O frame is bent (60.5°) and the water molecule is H-bonded to the OH group. The $IUOI$ isomer is the less stable of the three ($-1.7 \text{ kcal mol}^{-1}$), lacks of direct Ba-water interactions and the oxygen atom of the water molecule is H-bonded to the OH group. The $IUIO$ isomer is intermediate in energy ($-11.2 \text{ kcal mol}^{-1}$). The $IUIO$ structure lacks for H-bonds and the O-atom of water interacts directly with the Ba atom [$\angle(\text{O}–\text{Ba}–\text{O}) = 110.8^\circ$]. The $\text{Ba}–\text{OH}(\text{H}_2\text{O})_1$ distance gradually increases in the order $IUOI$, $IUIO$, and $IUII$ (2.19, 2.23 and 2.32 Å, respectively), and it is found that hydration structures of the $\text{HOBa}–\text{OH}_2$ type are much more stable than those of the $\text{BaOH}–\text{OH}_2$ type. The latter is also observed in higher order clusters ($m > 1$), which determines that the corresponding analogues to $IUOI$ having the $\text{BaOH}–\text{OH}_2$ structure are generally much less stable than the remaining stable isomers.

Four stable structures have been located on the potential energy surface (PES) of $\text{BaOH}(\text{H}_2\text{O})_2$. The most stable corresponds to the $2U22$ isomer ($-28.8 \text{ kcal mol}^{-1}$) with both water molecules directly bonded to the Ba atom and H-bonded to the OH group. In

addition, a cyclic isomer, *2U11*, with an energy difference of only 0.8 kcal mol⁻¹ with respect to the *2U22* isomer was found. This isomer exhibits only one Ba–O(H₂) interaction, and the second water molecule is bonded to both the former and the OH group by two H-bonds. The *2U20* isomer (-22.6 kcal mol⁻¹) has both water molecules directly bonded to the Ba atom and lacks for H-bonds. The corresponding (H₂)O–Ba–OH and (H₂)O–Ba–O(H₂) angles are 120.8° and 95.5°, respectively, with the Ba and the three O atoms in a nearly pyramidal geometry. The *2U02* isomer has a six-membered ring structure and it lacks for direct metal-water interactions. This fact probably accounts for its observed minor relative stability (-11.4 kcal mol⁻¹).

Nine stable structures have been characterized for the BaOH(H₂O)₃ cluster. The four more stable isomers (*3U12_b*, *3U22*, *3D33* and *3U32*) are essentially iso-energetic, with a relative energy difference < 0.8 kcal mol⁻¹. Out of them, the two lowest-energy isomers, namely, *3D33* and *3U32*, have the three water molecules bonded to barium atom and at least two H-bonds to the OH group. A higher-energy *3U11* isomer (-37.5 kcal mol⁻¹) has a cyclic structure with one Ba–O(H₂) interaction. The *3U20* isomer presents two water molecules bonded to the Ba atom, i.e., one more than *3U11*. The former isomer is 2 kcal mol⁻¹ less stable than the latter, probably because the third H-bonded water molecule in *3U20* can be affectively considered in the second hydration shell of Ba. The *3U12_a* (-30.6 kcal mol⁻¹) and *3U23* (-31.2 kcal mol⁻¹) isomers are related to *2U11* and *2U22*, respectively. Both add a water molecule that is H-bonded to the OH group. The *3U02* isomer was found to be the highest in energy (-21.4 kcal mol⁻¹), with a H-bonded ring structure between the OH group and the water molecules. As for the *2U02* isomer of BaOH(H₂O)₂, the lack of direct metal-water interactions in *3U02* could explain its lower stability with regard to the remaining BaOH(H₂O)₃ isomers.

The above results indicate that the sequential addition of water molecules to BaOH leads to increases in (i) the number of H-bonding interactions within the BaOH(H₂O)_m cluster, in (ii) the coordination number of both the Ba atom and the OH group, and in (iii) the Ba–OH bond distance that, compared to the value of 2.20 Å for bare BaOH, is 2.318 Å for *1U11* and 2.554 Å for *3U32*.

Such effects are accompanied by an increasing trend for the generation of stable dissociated isomers with increasing hydration. Whereas all of the lowest-energy isomers of BaOH(H₂O)_{1,2} clusters are undissociated, one stable low-energy isomer of BaOH(H₂O)₃ (*3D33*) is found to be dissociated (Ba–OH bond distance of 3.43 Å).

A larger number of stable dissociated species has been found for the most stable isomers of BaOH(H₂O)_{4,5} at the *mPW1PW91* level of theory (Figure 4). For these species the Ba–OH bond distance also increases with the hydration number, *e.g.*, 3.726 Å for *4D33* and 3.938 Å for *5D33_a*. In addition, the undissociated *4U22* and *5U22* isomers exhibit binding energies very close to those of the nearly iso-energetic, dissociated isomers. Seemingly, five solvent molecules do not lead to BaOH full dissociation.

5.3. Ionization energies of BaOH(H₂O)_m clusters

To calculate the adiabatic ionization energies of BaOH(H₂O)_m clusters, the corresponding cationic structures were optimized at the *mPW1PW91* level of theory. The derived geometries and CCSD(T,Full) binding energies are given in Figure 3. As for neutral clusters, the hydration in the BaOH⁺(H₂O)_m species is dominated by the direct coordination of the water molecules to the Ba atom center over formation of H-bonded networks involving the OH group. For example, the *1U11*⁺, *2U22*⁺, and *3U32*⁺ isomers, which exhibit water molecules bonded by Ba⁺–O interactions, are more stable

than the $1U01^+$, $2U01^+$ and $3U01^+$ isomers, which have a H_2O molecule H-bonded to the OH group.

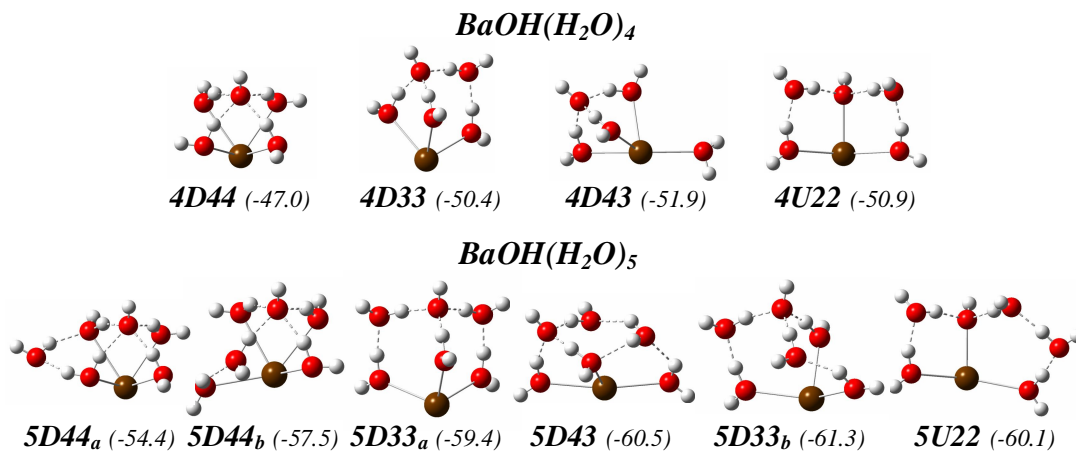


Figure 4. Same as Fig. 2, but for selected most stable $BaOH(H_2O)_m$ ($m = 4$ and 5) clusters. The binding energy (in $kcal\ mol^{-1}$) next to the label of each structure was calculated at $mPW1PW91$ level. The results show an increase in the number of dissociated stable geometries as a function of m .

Table I lists the vertical and adiabatic ionization energies for the $BaOH(H_2O)_m$ ($m = 0 - 3$) clusters derived from the DFT and the CCSD(T,Full) methods. As it can be seen, both levels of theory lead to very close IE_v and IE_a values for all m . A good agreement between the experimental and calculated IE 's is apparent, and the systematic decrease of IE_e 's with increasing size of the cluster is well reproduced. Noteworthy, such a trend is opposite to the reported behavior in previous theoretical studies of the $MOH(H_2O)_m$ ($M = Li, Na, K, Rb, Cs$) systems,¹⁴⁻¹⁷ for which the IE_v 's, as derived from the MP2 method were found to increase consistently with the number of water molecules. Unfortunately, no experimental data seems to be available to confirm the findings for the hydrated alkaline hydroxides.

A comparison between the experimental and predicted ionization energies for $\text{BaOH}(\text{H}_2\text{O})_m$ ($m = 0 - 3$) is relevant at this time. In fact, except for the *1U10* and *2U20* isomers, the IE_v 's for the mono-, di-, and tri-hydrated clusters are larger than the IE_e values. Instead, the calculated adiabatic ionization energies for the most stable $\text{BaOH}(\text{H}_2\text{O})_{1,2}$ clusters are very similar to the IE_e 's. The same holds for $\text{BaOH}(\text{H}_2\text{O})_3$ species except for their lowest-energy isomers.

The adiabatic ionization process for the less stable clusters involves a substantial geometry rearrangement of the ionic species. For example, the *ring* structure is broken upon the $2U02 + h\nu \rightarrow 2U01^+$ or $3U02 + h\nu \rightarrow 3U01_b^+$ processes. As a result, the adiabatic process for these clusters is likely to be spectroscopically unfavourable. Considering that the actual ionization process probably involves a structural relaxation of the ion to some extent, the computed IE_v 's can be seen as upper theoretical limits.

6. Discussion

6.1. Comparison of experimental and theoretical results

As abovementioned, the theoretical analysis shows that cluster structures with Ba-OH₂ bonds are mostly favoured. The quantum chemical results of Table I also indicate that the more energetic isomers probably do not account for the experimental data. In fact, the calculated IE_a 's for the *1U01*, *2U02*, and *3U02* configurations (4.28, 4.38, and 4.50 eV, respectively) are systematically higher than the IE_e 's (4.17, 3.91, and 3.76 eV).

Regarding the most stable isomers of the whole $\text{BaOH}(\text{H}_2\text{O})_m$ ($m=1$ to 3) set, the CCSD(T,Full) values for IE_v and IE_a are close to the experimentally measured values. This is the case of the *1U11* isomer, for which $\text{IE}_e = 4.17 \pm 0.05$ eV lies between the calculated IE_v (4.32 eV) and IE_a (4.14 eV). On the contrary, the computed IE_v and IE_a

for the *IUIO* isomer of 4.05 and 4.01 eV, respectively, are somewhat lower than the photoionization threshold for $\text{BaOH}^+(\text{H}_2\text{O})_1$ ions at 4.17 eV. On this basis, it is suggested that the *IUII* isomer is the most populated $\text{BaOH}(\text{H}_2\text{O})_1$ cluster of this series in the molecular beam.

The lowest IE_e for $\text{BaOH}(\text{H}_2\text{O})_2$ at 3.80 eV could be certainly assigned to the adiabatic photoionization of the *2U22* isomer. While the lowest IE_e also coincides with the CCSD(T,Full) IE_v (3.80 eV) of the *2U20* isomer, the present calculations show that the corresponding $2U20^+$ structure is unstable. Besides, the expected population of the *2U20* isomer in the molecular beam is much lower than that of the most stable isomer *2U22*. Even if the *2U20* isomer is present in the molecular beam, its vertical photoionization would imply a strong reorganization in the formed cationic cluster, thereby turning unlikely the whole processes. This fact, along with the lack of observation for an IE_e feature similar to the IE_a of *2U20* (3.63 eV), suggests that this isomer may be at least a minor component in the molecular beam.

A rationalization of the higher-energy IE_e for $\text{BaOH}(\text{H}_2\text{O})_2$ at 3.91 eV should be addressed. Whereas this is in agreement with the IE_a value for the *2UII* isomer, alternative assignments cannot be excluded at present. The latter include the presence in the molecular beam of two low-lying vibrational states of a given isomer for $\text{BaOH}(\text{H}_2\text{O})_2$, as well as the promotion of a given neutral isomer in its vibrational ground-state to two different low-lying vibrational states of its cationic form upon photoionization. Indeed, the energy difference of (0.11 ± 0.07) eV [(887 ± 565) cm^{-1}] between the two lowest IE_e 's for $\text{BaOH}(\text{H}_2\text{O})_2$ lies within the energy range of vibrational quanta, which are associated to 7-8 normal modes for all of the isomers involved in the $2U22 + h\nu \rightarrow 2U22^+$ and $2UII + h\nu \rightarrow 2U21^+$ processes, as derived from the present calculations. Hence, the discussion hereafter will rely on considering

the lowest IE_e for $BaOH(H_2O)_2$ alone which, as mentioned above, is in agreement with the IE_a value of the $2U22$ isomer.

The above considerations hold true for $BaOH(H_2O)_3$ as well, on the basis of comparing the (0.06 ± 0.06) eV [(484 ± 484) cm^{-1}] energy difference between its two lowest IE_e 's and the values of the calculated harmonic vibrational frequencies for the relevant isomers. Hence, only the lowest IE_e for $BaOH(H_2O)_3$ will be considered hereafter. The CCSD(T,Full) computed IE_v and IE_a values for three out of nine $BaOH(H_2O)_3$ isomers agree with the lowest IE_e at 3.70 eV. Because the estimated IE_a (4.50 eV) of the highest-energy $3U02$ species is 0.8 eV higher than the IE_e 's, this isomer could be, in principle, discarded. It is interesting to focus now on the group of the most stable, near iso-energetic isomers ($\Delta E_0 \approx -42$ kcal mol⁻¹): $3U12_b$, $3U22$, $3D33$, and $3U32$. Whereas the adiabatic IE (3.73 eV) of the $3U22$ isomer agrees with the lowest IE_e within the assigned uncertainty (0.05 eV), the IE_a 's for the remaining isomers are very similar, ~ 3.54 eV, and in all cases somewhat lower than relevant IE_e . Regarding the remaining four isomers, *i.e.*, $3U12_a$, $3U23$, $3U20$, and $3U11$, only $3U12_a$ and $3U23$ have IE_a values of 3.70 eV and 3.68 eV, respectively, in agreement with the relevant IE_e . Therefore, an unambiguous assignment of the lowest IE_e for $BaOH(H_2O)_3$ clusters to an adiabatic or vertical photoionization process of any predicted isomer does not appear to be possible.

Figure 5 compares the lowest IE_e 's with the theoretical IE_v 's and IE_a 's values of the relevant $BaOH(H_2O)_m$ clusters, as derived from the CCSD(T,Full) method: Overall, there is a good agreement between the IE_e 's and the calculated IE_a 's for such isomers.

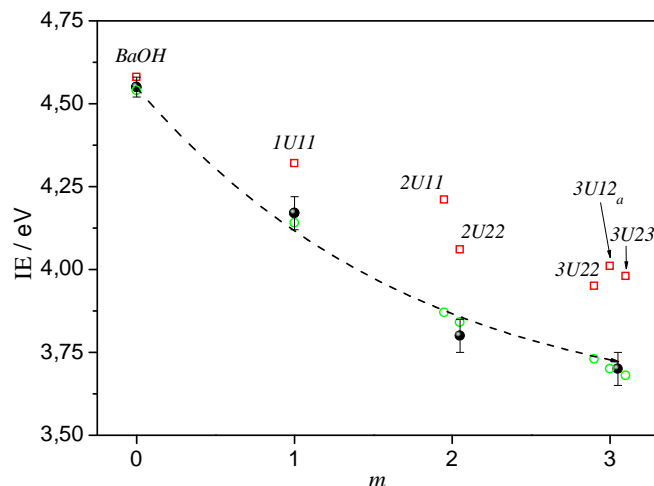


Figure 5. Experimental and calculated IE's for $\text{BaOH}(\text{H}_2\text{O})_m$ ($m = 0 - 3$) clusters as a function of m . (●): lowest experimental IE_e ; (□): vertical IE_v ; (○): adiabatic IE_a . The theoretical values correspond to the structures highlighted on Table I.

6.2. BaOH solvation in $(\text{H}_2\text{O})_m$ ($m = 1 - 5$) clusters

The present results indicate that the sequential attachment of water molecules to BaOH changes its linear geometry to some extent (see Figure 2) as well as the Ba-OH bond length. This is a consequence of the changes in the local charges of the Ba and O atoms in BaOH, and thus to the polarization of the Ba-OH bond, as induced by the water molecules.

The strong $\text{Ba}^+(\text{OH})^-$ ionic character of the BaOH radical is observed in all of the $\text{BaOH}(\text{H}_2\text{O})_m$ clusters. To obtain reliable estimates of the charge distribution on the Ba and O atoms of the BaOH radical, a natural population analysis on the characterized clusters was carried out. The resulting values are listed in Fig. 2. It is apparent that the charges change slightly when the O atom of the water molecule is H-bonded to OH group. For the weakly-bonded *1U01* complex, a Ba-OH bond length decrease of 0.013 Å respect to bare BaOH is observed. Instead, the O atom charge in BaOH becomes less negative when the OH group acts as a proton acceptor. This is the case for the *1U11*

isomer of $\text{BaOH}(\text{H}_2\text{O})_1$. As a result of strong HO-HOH and Ba-OH₂ interactions, *IU11* is most stable ($\Delta E_0 = -14.2 \text{ kcal mol}^{-1}$) than *IU01*, and displays a Ba-OH bond polarization decrease and a Ba-OH bond distance increase of 0.114 Å.

Figure 6 shows relaxed PES scans performed at the *mPW1PW91* level for selected neutral $\text{BaOH}(\text{H}_2\text{O})_m$ species as a function of the Ba-OH bond distance. As expected, the dissociation of bare BaOH is a barrierless process having a well depth (D_e) of 125.9 kcal mol⁻¹ [Figure 6 (a)]. On the other hand, for $\text{BaOH}(\text{H}_2\text{O})_m$ ($m = 1 - 5$) clusters, a H-transfer from one water molecule to the OH group leads to a H₂O elimination channel, *i.e.*, $\text{BaOH}(\text{H}_2\text{O})_{m-1} + \text{H}_2\text{O}$, instead of the competitive OH elimination $\text{Ba}(\text{H}_2\text{O})_m + \text{OH}$. This is illustrated in Figures 6 (b) and (c) for the *3D33* and *5D33_a* isomers of the $\text{BaOH}(\text{H}_2\text{O})_3$ and $\text{BaOH}(\text{H}_2\text{O})_5$ clusters. Upon H₂O elimination, the resulting species, $\text{BaOH}(\text{H}_2\text{O})_2$ and $\text{BaOH}(\text{H}_2\text{O})_4$ are stabilized by 14.0 and 2.3 kcal mol⁻¹ with respect to the highest energy point along the reaction coordinate. These results indicate that, despite the Ba-OH bond distance increases with m , five solvent molecules are not enough to fully dissociate the BaOH radical. Overall, the present experimental and theoretical results for $\text{BaOH}(\text{H}_2\text{O})_m$ together with results of previous theoretical studies related to the $\text{MOH}(\text{H}_2\text{O})_m$ ($M = \text{Li, Na, K, Rb, Cs}$) systems,¹⁴⁻¹⁷ allow estimates in the number of water molecules which seem to be required for full dissociation of the relevant metal monohydroxides: $m > 5$ for BaOH, 7 for LiOH,¹⁶ 6 for NaOH and KOH,¹⁷ 5 for RbOH,¹⁵ and 4 for CsOH.¹⁴

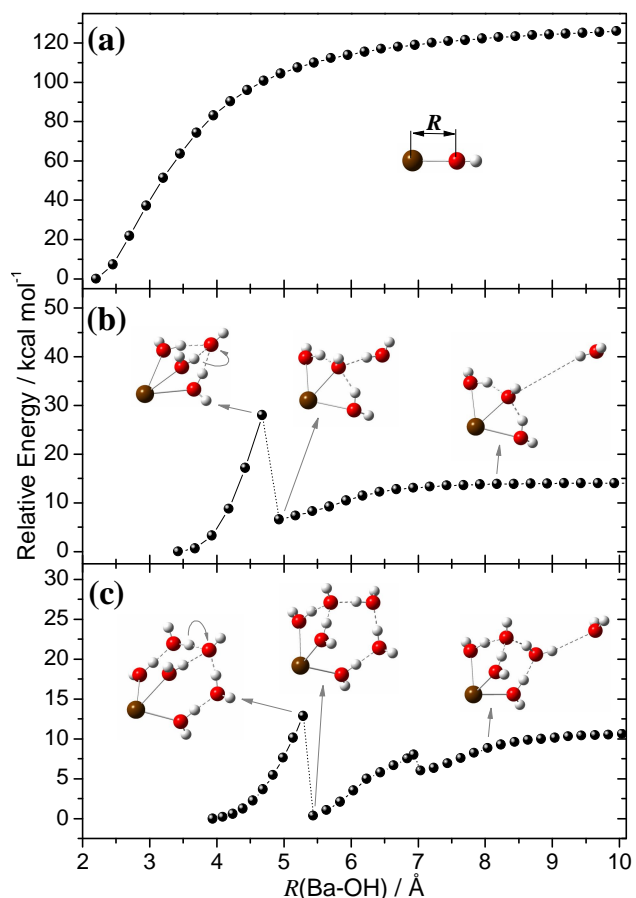


Figure 6. Potential energy curves calculated at the *m*PW1PW91 level, for the ground neutral state of $\text{BaOH}(\text{H}_2\text{O})_m$ as a function of the Ba-OH bond length (from the equilibrium distance, R_0). (a): $m = 0$, BaOH; (b): $m = 3$, $3D33$ isomer; (c): $m = 5$, $5D33_a$ isomer.

6.3. Solvation of BaOH vs Ba and MOH (M = Li, Na, K, Rb, Cs) in water clusters

A theoretical energy level diagram of the hydration energies for the relevant BaOH- and Ba-doped water clusters, for both neutral and cationic species is depicted in Figure 7. It is apparent that the hydration energies of $\text{BaOH}(\text{H}_2\text{O})_m$ clusters are larger than those of $\text{Ba}(\text{H}_2\text{O})_n$ species for $m = n$, e.g., the E_{hyd} 's for BaOH-H₂O (14.2 kcal mol⁻¹) and BaOH(H₂O)-H₂O (14.5 kcal mol⁻¹) are larger than those for Ba-H₂O (11.2 kcal mol⁻¹) and Ba(H₂O)-H₂O (12.3 kcal mol⁻¹). A similar trend is observed by comparing the hydration energies of $\text{BaOH}^+(\text{H}_2\text{O})_m$ and $\text{Ba}^+(\text{H}_2\text{O})_n$ clusters, which are found to be about twice those for the corresponding neutral species. All findings can be

rationalized on the basis of the results of the natural population analysis performed here for neutral and cationic $\text{BaOH}(\text{H}_2\text{O})_m$ clusters, and previously⁷ for the corresponding $\text{Ba}(\text{H}_2\text{O})_n$ species. Indeed, Figs. 2 and 3 show that the $\text{BaOH}/\text{BaOH}^+$ cores of all neutral/cationic clusters are significantly polarized, with effective charges of $-(1.2-1.4)$ on the O atom of the OH group and of $+(0.9-1.0)/+(1.8-1.9)$ on the Ba atom of $\text{BaOH}(\text{H}_2\text{O})_m/\text{BaOH}^+(\text{H}_2\text{O})_m$ clusters. This situation contrasts with the relatively low Ba atom charges of $+(0.03-0.20)$ in $\text{Ba}(\text{H}_2\text{O})_n$ ($n = 1-4$) clusters, and of around $+(1.0)$ in $\text{Ba}^+(\text{H}_2\text{O})_n$. The relatively strong polarization of the BaOH and BaOH^+ cores strengthens the bonding with water molecules as compared to the Ba and Ba^+ cases, which in turn determines that the E_{hyd} 's of all $\text{BaOH}(\text{H}_2\text{O})_m/\text{BaOH}^+(\text{H}_2\text{O})_m$ clusters are much larger than those of $\text{Ba}(\text{H}_2\text{O})_n/\text{Ba}^+(\text{H}_2\text{O})_n$ for $m = n$. Similar trends have been found by Watanabe *et al.*^{19,20} for the reactions between Mg^+ and Ca^+ ions with $(\text{H}_2\text{O})_n$ clusters. These theoretical studies were aimed to explain previous experimental observations that $\text{M}^+(\text{H}_2\text{O})_n$ species are predominantly produced for $n \leq 5$ and 4 for Mg^+ and Ca^+ , respectively, whereas the $\text{MOH}^+(\text{H}_2\text{O})_{n-1}$ products dominate in the ranges of 6-14 and 5-13, respectively.

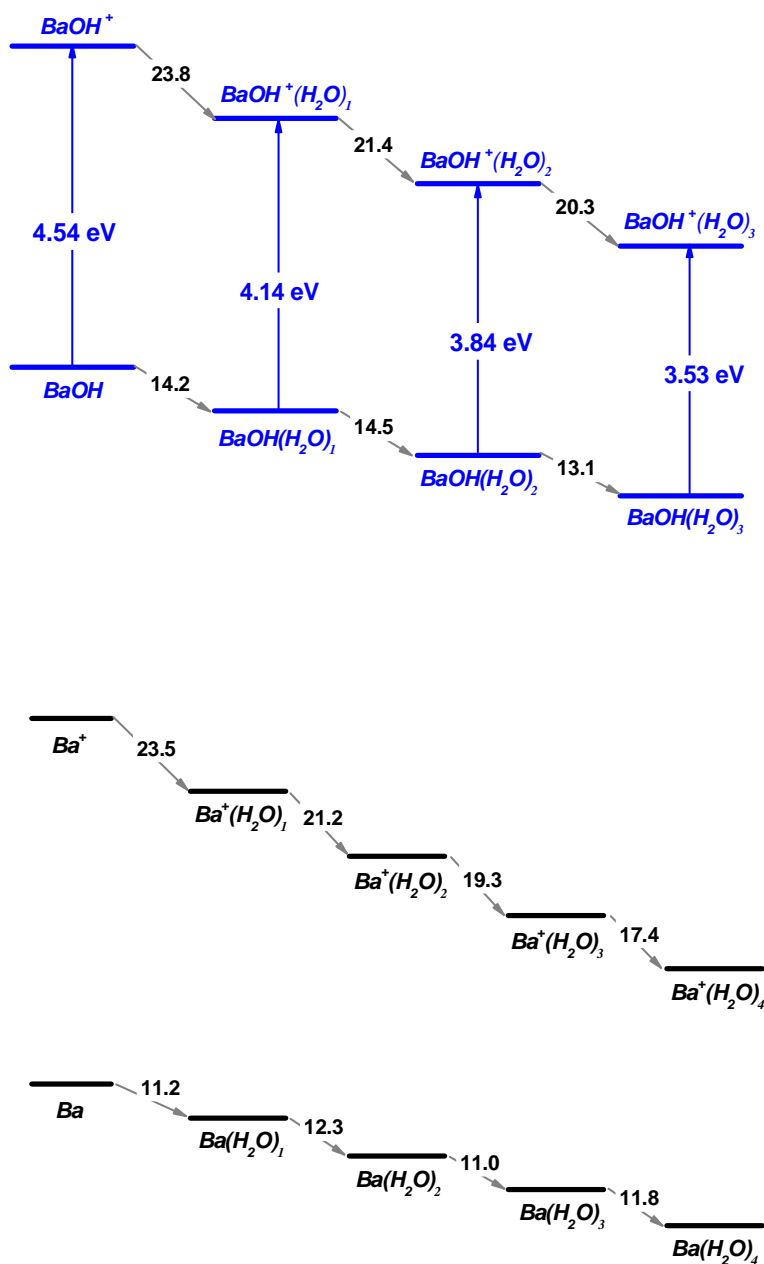


Figure 7. Theoretical energy level diagram performed at the CCSD(T,Full)//mPW1PW91 level, for hydration of BaOH (upper plot) and Ba (lower plot; extracted from Ref. 7), in the neutral and cationic states. Grey diagonal arrows are the hydration energies (E_{hyd}) in kcal mol⁻¹, and blue vertical arrows are the adiabatic ionization energies (IE_a) in eV. The most stable isomer for each cluster was used.

A further insight into the stepwise hydration behaviour of the BaOH radical could be gained from comparing the cluster size dependence of the theoretical IE_v 's for the most stable isomers of $BaOH(H_2O)_m$ ($m = 0-3$) clusters, with the corresponding values for the $MOH(H_2O)_m$ ($M = Li, Na, K, Rb, Cs$) systems, as derived from MP2 calculations by Kim and co-workers.¹⁴⁻¹⁷ Despite the lack of CCSD(T,Full) IE_v 's for the hydrated alkali monohydroxides does not allow for a straightforward comparison to be made with the corresponding values for the title system, it was found that the IE_v 's for the most stable $MOH(H_2O)_m$ ($M = \text{alkaline metal}$) isomers generally increase with the number of water molecules, which is opposite to the trends found for $BaOH(H_2O)_m$. The differing behaviours may be rationalized considering the nature of the photoionization process in bare BaOH and MOH first. Owing to the highly ionic character of the Ba–OH and M–OH bonds, ionization in such species can be envisaged as electron removal either from the Ba^+/M^+ or the OH^- moieties. The former is true in the case of BaOH, for which removal of the unpaired electron in its ground state occurs from a nonbonding orbital located primarily on the Ba^+ ion core and polarized away from the OH^- ion,²¹ whereas ionization of MOH (and other closed-shell alkaline hydroxides) corresponds essentially to removal of the electron from the OH^- moiety.²⁸ This picture is likely to hold for $BaOH(H_2O)_m$ clusters considering the effective charges on the Ba atom for $BaOH(H_2O)_m$ and $BaOH^+(H_2O)_m$ (Figs. 2 and 3), *i.e.*, the ionization process can be considered as $[Ba^+OH^-(H_2O)_m] + h\nu \rightarrow [Ba^{2+}OH^-(H_2O)_m]^+ + e^-$. As the number m of water molecules increases, the solvation of the neutral $BaOH(H_2O)_m$ clusters is not as strong as for the corresponding ions $BaOH^+(H_2O)_m$, because of the stronger charge-charge and charge-dipole interactions that are at play between the Ba^{2+} and $OH^-(H_2O)_m$ cores in the ionic clusters. In turn, this will lead to a decrease in the ionization energy of $BaOH(H_2O)_m$ with increasing cluster size. The opposite picture holds in the case of

CsOH(H₂O)_m clusters, for which the ionization process can be considered as [Cs⁺OH⁻(H₂O)_m] + *hν* → [Cs⁺OH(H₂O)_m]⁺ + *e*⁻, thereby resulting in stronger charge-charge and charge-dipole interactions at play between the Cs⁺ and OH⁻(H₂O)_m cores in the neutral clusters than in cationic clusters, and leading to an increase in the CsOH(H₂O)_m ionization energy with increasing cluster size.

The above considerations bring out the significance of the open-shell nature of BaOH in determining the hydration structures and electronic properties of small BaOH-doped water clusters, as compared to the closed-shell MOH(H₂O)_m (M = Li, Na, K, Rb, Cs)¹⁴⁻¹⁸ and MOH⁺(H₂O)_m (M = Mg, Ca)¹⁹⁻²⁰ systems. For the latter, electrostatic interactions dominate the bonding of MOH/MOH⁺ to water molecules. This is revealed by the finding for hydrated alkali monohydroxides, that a fully dissociated conformation is usually attained as the number of solvating water molecules is large enough, so as to tricoordinate the OH⁻ moiety with water molecules. Instead, the required hydration number for the series of isovalent M⁺ moieties, having a closed-shell spherical electron distribution, depends chiefly on their charge-to-radius ratio and generally decreases with the corresponding atomic mass.¹⁴⁻¹⁸

As pointed out above, electrostatic interactions contribute significantly to bonding between the strongly polarized BaOH radical and the water molecules as well. Notwithstanding, inductive effects on the BaOH unpaired electron distribution should be considered in order to address the different dissociation behavior in (H₂O)_m clusters with respect to the alkali monohydroxides,¹⁴⁻¹⁸ especially CsOH that seems to require a smaller number of water molecules for full dissociation (*m* = 4), as compared to BaOH (*m* > 5). The difference might be explained in terms of the effect that the successive binding of water molecules to BaOH is expected to have on the electron distribution around its Ba⁺ moiety. In bare ground-state BaOH, a polarized electron density on the

opposite side of the barium atom from the OH^- moiety is predicted to result from repulsion between the unpaired electron and the electron cloud of the OH^- moiety. In analogy with the alkaline earth monohalides,²⁹ such a polarization is achieved through $6s\sigma$ - $6p\sigma$ orbital mixing on the barium atom, which produces a nonbonding orbital where the BaOH 's valence (unpaired) electron resides. This is corroborated by additional calculations on the electron density distribution of the singly occupied molecular orbital (SOMO) for bare BaOH (Figure 8). Within this picture, a fully dissociated conformation in $\text{BaOH}(\text{H}_2\text{O})_m$ clusters is expected to develop upon attainment of spatial charge polarization¹⁸ of the hydrated Ba^+ and OH^- moieties, along with delocalization to some extent of the corresponding unpaired electron over the surrounding water molecules. Figure 8 shows theoretical results on the SOMO's for the most stable isomers of $\text{BaOH}(\text{H}_2\text{O})_{1-5}$ clusters as well. These SOMO's extend in a large vacant space around the barium atom and in a direction perpendicular to the Ba-OH bond, which indicates that they retain a nonbonding character upon sequential solvation by less than five water molecules. Most significantly, these unpaired electron density distributions are chiefly polarized away from the electron clouds on the oxygen atoms of both the water molecules and the OH^- moieties, which for all cluster sizes are found to be more negative than the oxygen atom of bare H_2O (Fig. 2). This is especially true for the oxygen atoms of the OH^- moieties, which in turn suggests that, despite the Ba-OH bond distance increases with the cluster size (see Sec. 6.2), the OH^- ion exerts a major influence on the Ba^+ counterion, to the extent that the valence electron of the most stable $\text{BaOH}(\text{H}_2\text{O})_{1-5}$ isomers do not effectively delocalize over such small water clusters. As a result, these hydrated OH^- moieties might be thought of interacting with nearby, closed-shell Ba^{2+} ion cores that are partially shielded by their (valence) electron clouds. The latter is expected to lead to stronger charge-dipole interactions with water

molecules, as compared to the Cs^+ ion case, which in turn would explain the relatively large hydration numbers that are required for dissociating the BaOH radical into spatially polarized Ba^+ and OH^- moieties.

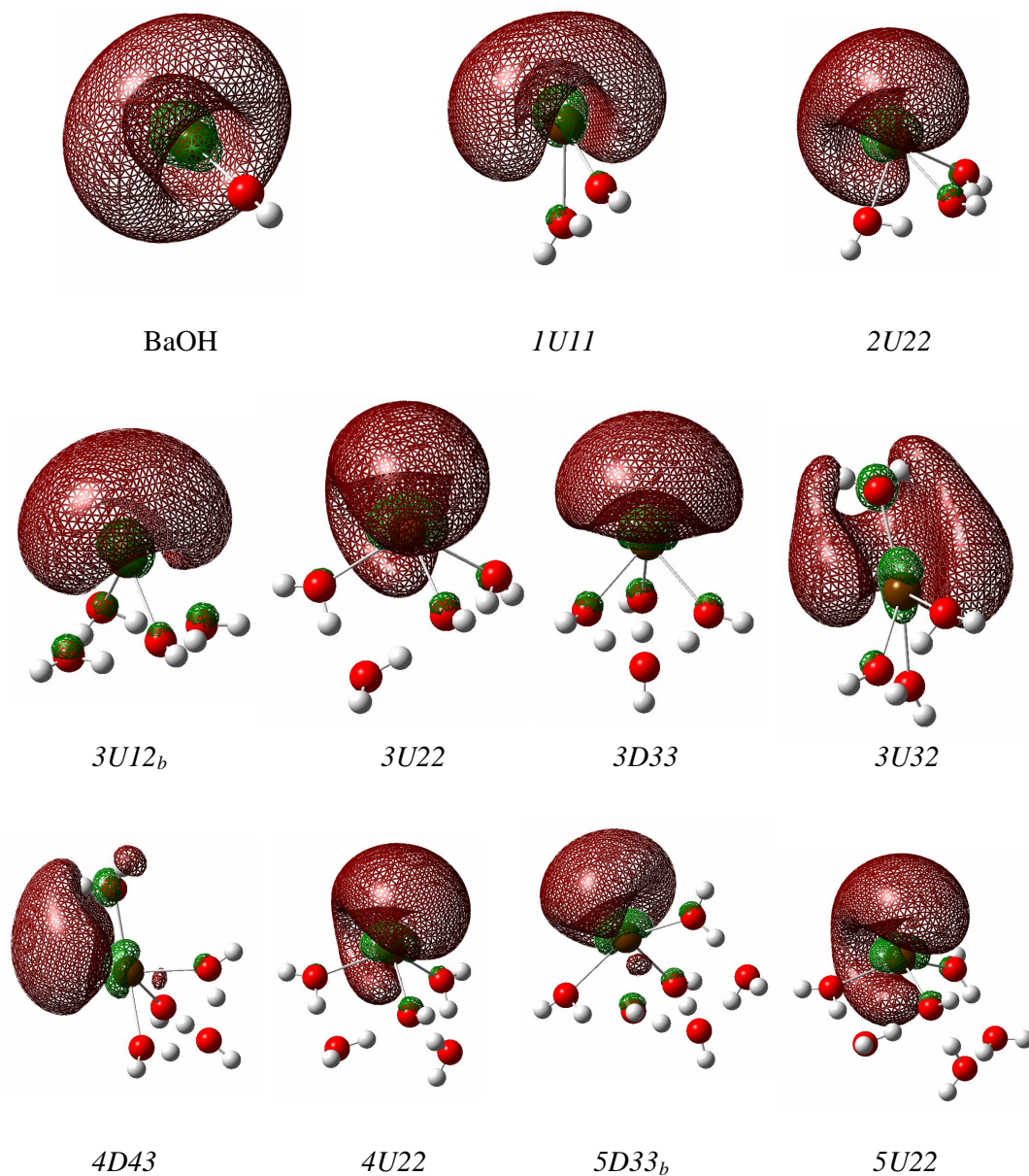


Figure 8. Electronic density distribution of the SOMO in $\text{BaOH}(\text{H}_2\text{O})_m$ clusters ($m = 0 - 5$). The iso-density surfaces correspond to 0.03 \AA^{-3} .

7. Concluding remarks

The present work reports the determination in laser one-photon ionization experiments of the ionization energies of $\text{BaOH}(\text{H}_2\text{O})_m$ ($m = 1-3$) clusters. Complementary *ab initio* calculations show that the experimental values are in good agreement with a chiefly adiabatic ionization process, while they allow for an assessment of the most likely BaOH hydration structures under the prevailing experimental conditions. Both the experimental and theoretical IE's for the open-shell $\text{BaOH}(\text{H}_2\text{O})_m$ clusters decrease with the number of water molecules, which is opposite to the trends reported for the IE's of the closed-shell $\text{MOH}(\text{H}_2\text{O})_m$ ($M = \text{Li, Na, K, Rb, Cs}$) systems. On the basis of calculated hydration energies, atom-charge and valence-electron distributions for the most stable isomers of $\text{BaOH}(\text{H}_2\text{O})_m$ clusters with up to $m = 5$, it was shown that the opposite behaviours is a consequence of the different electrons that are removed upon photoionization: The unpaired electron on the Ba^+ moiety for BaOH and an electron of the OH^- moiety for closed-shell MOHs. Overall, the present evidence is compatible with an increasing solvation of the Ba^+ and OH^- ion cores upon sequential addition of a small number of water molecules to BaOH, and it is also suggestive for the initial steps of the BaOH hydration process to be dominated by $\text{Ba}^+ - \text{OH}^-$ electrostatic and polarization interactions.

Acknowledgments

This work was supported by CONICET, FONCyT, SeCyT-UNC and MinCyT Córdoba. I. C.-V. and M. R. acknowledge post-doctoral fellowships from CONICET-Argentina.

References

- (1) Campargue, R. *Atomic and Molecular Beams: The State of the Art 2000*; Springer: Berlin, 2001.
- (2) Stace, A. *Cluster Solutions Science* **2001**, 294, 1292-1293.
- (3) Farrar, J. J. Size-Dependent Reactivity in Open Shell Metal-Ion Polar Solvent Clusters: Spectroscopic Probes of Electronic-Vibration Coupling, Oxidation and Ionization *Int. Rev. Phys. Chem.* **2003**, 22, 593-640.
- (4) Abel, B.; Buck, U.; Sobolewski, A. L.; Domcke, W. On the Nature and Signatures of the Solvated Electron in Water *Phys. Chem. Chem. Phys.* **2012**, 14, 22-34.
- (5) Okai, N.; Ishikawa, H.; Fuke, K. Hydration Process of Alkaline-Earth Metal Atoms in Water Clusters *Chem. Phys. Lett.* **2005**, 415, 155-160.
- (6) Cabanillas-Vidosa, I.; Rossa, M.; Pino, G. A.; Ferrero, J. C. Unexpected Size Distribution of $\text{Ba}(\text{H}_2\text{O})_n$ Clusters: Why is the Intensity of the $\text{Ba}(\text{H}_2\text{O})_1$ Cluster Anomalous Low? *Phys. Chem. Chem. Phys.* **2011**, 13, 13387-13394.
- (7) Cabanillas-Vidosa, I.; Rossa, M.; Pino, G. A.; Ferrero, J. C.; Cobos, C. J. Photoionization and *Ab Initio* Study of $\text{Ba}(\text{H}_2\text{O})_n$ ($n = 1 - 4$) Clusters *Phys. Chem. Chem. Phys.* **2012**, 14, 4276-4286.
- (8) Misaizu, F.; Sanekata, M.; Tsukamoto, K.; Fuke, K.; Iwata, S. Photodissociation of Size-Selected $\text{Mg}^+(\text{H}_2\text{O})_n$ Ions for $n = 1$ and 2 *J. Phys. Chem.* **1992**, 96, 8259-8264.
- (9) Misaizu, F.; Sanekata, M.; Fuke, K.; Iwata, S. Photodissociation Study on $\text{Mg}^+(\text{H}_2\text{O})_n$, $n = 1-5$: Electronic Structure and Photoinduced Intracluster Reaction *J. Chem. Phys.* **1994**, 100, 1161-1170.
- (10) Sanekata, M.; Misaizu, F.; Fuke, K. Photodissociation Study on $\text{Ca}^+(\text{H}_2\text{O})_n$, $n = 1-6$: Electron Structure and Photoinduced Dehydrogenation Reaction *J. Chem. Phys.* **1996**, 104, 9768-9778.

- (11) Sperry, D. C.; Midey, A. J.; Lee, J. I.; Qian, J.; Farrar, J. M. Spectroscopic Studies of Mass Selected Clusters of Sr^+ Solvated by H_2O and D_2O *J. Chem. Phys.* **1999**, 111, 8469-8480.
- (12) Blades, A. T.; Jayaweera, P.; Ikononou, M. G.; Kebarle, P. Studies of Alkaline Earth and Transition Metal M^{++} Gas Phase Ion Chemistry *J. Chem. Phys.* **1990**, 92, 5900-5906.
- (13) Peschke, M.; Blades, A. T.; Kebarle, P. Hydration Energies and Entropies for Mg^{2+} , Ca^{2+} , Sr^{2+} , and Ba^{2+} from Gas-Phase Ion-Water Molecule Equilibria Determinations *J. Phys. Chem. A* **1998**, 102, 9978-9985.
- (14) Odde, S.; Pak, C.; Lee, H. M.; Kim, K. S.; Mhin, B. J. Aqua Dissociation Nature of Cesium Hydroxide *J. Chem. Phys.* **2004**, 121, 204-208.
- (15) Odde, S.; Lee, H. M.; Kolaski, M.; Mhin, B. J.; Kim, K. S. Dissolution of a Base (RbOH) by Water Clusters *J. Chem. Phys.* **2004**, 121, 4665-4670.
- (16) Veerman, A.; Lee, H. M.; Kim, K. S. Dissolution Nature of the Lithium Hydroxide by Water Molecules *J. Chem. Phys.* **2005**, 123, 084321.
- (17) Kumar, A.; Park, M.; Huh, J. Y.; Lee, H. M.; Kim, K. S. Hydration Phenomena of Sodium and Potassium Hydroxides by Water Molecules *J. Phys. Chem. A* **2006**, 110, 12484-12493.
- (18) Roy, D. R. Theoretical Study of Microscopic Solvation of NaOH in Water: $\text{NaOH}(\text{H}_2\text{O})_n$, $n = 1-10$ *Chem. Phys.* **2012**, 407, 92-96.
- (19) Watanabe, H.; Iwata, S.; Hashimoto, K.; Misaizu, F.; Fuke, K. Molecular Orbital Studies of the Structures and Reactions of Singly Charged Magnesium Ion with Water Clusters, $\text{Mg}^+(\text{H}_2\text{O})_n$ *J. Am. Chem. Soc.* **1995**, 117, 755-763.

- (20) Watanabe, H.; Iwata, S. Molecular Orbital Studies of the Structures and Reactions of a Singly Charged Calcium Ion with Water Clusters, $\text{Ca}^+(\text{H}_2\text{O})_n$ *J. Phys. Chem. A* **1997**, 101, 487-496.
- (21) Rossa, M.; Cabanillas-Vidosa, I.; Pino, G. A.; Ferrero, J. C. New Determination of the Adiabatic Ionization Potential of the BaOH Radical from Laser Photoionization-Molecular Beam Experiments and *Ab Initio* Calculations *J. Chem. Phys.* **2012**, 136, 0643031-0643038.
- (22) Adamo, C.; Barone, V. Exchange Functionals with Improved Long-Range Behavior and Adiabatic Connection Methods Without Adjustable Parameters: The mPW and mPW1PW Models *J. Chem. Phys.* **1998**, 108, 664-675.
- (23) Bartlett, R. J. Many-Body Perturbation Theory and Coupled Cluster Theory for Electron Correlation in Molecules *Annu. Rev. Phys. Chem.* **1981**, 32, 359-401.
- (24) Raghavachari, K.; Trucks, G. W.; Pople, J. A.; Head-Gordon, M. A Fifth-Order Perturbation Comparison of Electron Correlation Theories *Chem. Phys. Lett.* **1989**, 157, 479-483.
- (25) Lim, I. S.; Stoll, H.; Schwerdtfeger, P. Relativistic Small-Core Energy-Consistent Pseudopotentials for the Alkaline-Earth Elements from Ca to Ra *J. Chem. Phys.* **2006**, 124, 0341071-0341079.
- (26) Frisch, M. J.; Trucks, G. W.; Schlegel, H. B.; Scuseria, G. E.; Robb, M. A.; Cheeseman, J. R.; Scalmani, G.; Barone, V.; Mennucci, B.; Petersson, G. A.; *et al.* *Gaussian 09*, Revision A.02; Gaussian, Inc.: Wallingford, CT, 2009.
- (27) Kinsey-Nielsen, S.; Brazier, C. R.; Bernath, P. F. Rotational Analysis of the $B^2\Sigma^+ - X^2\Sigma^+$ Transition of BaOH and BaOD *J. Chem. Phys.* **1986**, 84, 698-708.
- (28) Lee, E. P. F.; Wright, T. G. Heats of Formation of NaOH and NaOH^+ : Ionization Energy of NaOH *J. Phys. Chem. A* **2002**, 106, 8903-8907.

(29) Ellis, A. M. Main Group Metal-Ligand Interactions in Small Molecules: New Insights from Laser Spectroscopy *Int. Rev. Phys. Chem.* **2001**, 20, 551-590.